Available online at www.sciencedirect.com
ScienceDirect
Construction and Building Materials 21 (2007) 1001–1010
Construction and Building MATERIALS
www.elsevier.com/locate/conbuildmat

Proposed design guidelines for strengthening of steel bridges with FRP materials

D. Schnerch [a], M. Dawood [b,*], S. Rizkalla [b], E. Sumner [b]

[a] *Wiss, Janney, Elstner Associates Inc., 245 First Street, Suite 1200, Cambridge, MA 02142, United States*
[b] *Constructed Facilities Laboratory, North Carolina State University, 2414 Campus Shore Dr., Campus Box 7533, Raleigh, NC 27695-7533, United States*

Received 13 September 2005; received in revised form 17 February 2006; accepted 8 March 2006
Available online 18 May 2006

Abstract

This paper focuses on the use of externally bonded high modulus carbon fiber reinforced polymer (HM CFRP) materials to strengthen steel bridges and structures. Proper installation of the CFRP materials is necessary to prevent premature failure due to debonding. The paper proposes guidelines and installation techniques based on the best practice reported in the literature and the extensive practical experience in bonding of composite materials. The surface preparation of the materials, the application of the adhesive and the detailing of the strengthening are provided in detail. The design guidelines include the structural design criteria for the use of high modulus CFRP materials as flexural strengthening system of typical steel–concrete composite bridge girders. The flexural design procedure is based on a moment–curvature analysis and a specified increase of the live load carried by the bridge to satisfy specific serviceability requirements. A bond model is also described which can be used to calculate the shear and peel stresses within the adhesive thickness. To prevent a premature debonding failure of the strengthening system, the criteria specify a maximum principle stress in the adhesive which cannot be exceeded for a given characteristic strength of an adhesive. A worked example is presented to illustrate the proposed flexural design approach. The research findings conclude that high modulus CFRP materials provide a promising alternative for strengthening steel bridges that can be easily designed and installed to increase their strength and stiffness.

Keywords: High modulus carbon fiber reinforced polymers; Steel structures; Design guidelines

1. Introduction

Due to increasing traffic loads and deterioration of steel bridges, there is a need to develop a cost-effective, durable strengthening system that can be used for the repair and strengthening of steel and steel–concrete composite bridge girders. Fiber reinforced polymer (FRP) materials have been widely used for the repair and strengthening of concrete bridges and structures. Due to the success of this technique, a number of researchers have investigated the use of carbon fiber reinforced polymer (CFRP) materials for repair and strengthening of steel [1] and steel–concrete composite [2–5] bridge girders. Most of the previous studies focused on the use of conventional modulus CFRP materials, which was found to be effective in increasing the ultimate capacity of steel and steel–concrete composite bridge girders. Due to the relatively low elastic modulus of the CFRP materials as compared to steel, a substantial amount of CFRP material was required to obtain significant stiffness increases.

Recently, high modulus CFRP (HM CFRP) materials have been developed with a tensile modulus approximately twice that of steel. A strengthening system using high modulus CFRP materials was developed at the Constructed Facilities Laboratory at North Carolina State University to increase the ultimate strength and stiffness of steel–concrete composite bridge girders. For this system, an appropriate adhesive was selected to bond the HM CFRP materials to steel based on a series of small-scale flexural

* Corresponding author. Tel.: +1 919 513 2040; fax: +1 919 513 1765.
E-mail address: mmdawood@ncsu.edu (M. Dawood).

0950-0618/$ - see front matter © 2006 Elsevier Ltd. All rights reserved.
doi:10.1016/j.conbuildmat.2006.03.003

tests [6]. The effectiveness of using prestressed HM CFRP strips to increase the stiffness of steel–concrete composite beams was demonstrated using a large-scale steel–concrete composite beam test [6]. The work at NC State University included a series of scale steel–concrete composite beams subjected to overloading and fatigue loading conditions [7]. The test results indicated superior performance of the strengthened beams under overloading and fatigue loading conditions as compared to unstrengthened beams tested in a similar configuration.

Based on the demonstrated superior performance of HM CFRP materials in strengthening steel–concrete composite beams, a series of installation and design guidelines were developed [8]. These guidelines were prepared using the best practice techniques reported in the literature, simple analytical tools and extensive experience in using HM CFRP materials for strengthening steel structures. This paper summarizes these guidelines, which can be used by practitioners for the design, analysis and installation of HM CFRP materials for strengthening of steel bridge girders.

2. HM CFRP strengthening system

High modulus carbon fiber materials have a modulus of elasticity approximately three times that of steel. The fibers are typically fabricated into pultruded laminate plates that are bonded to steel structures as an external reinforcement using an epoxy adhesive. This system provides an increase of the strength and stiffness, and therefore can be used to upgrade existing steel bridges. Typical material properties for the high modulus carbon fibers and the pultruded HM CFRP strips are provided in Table 1.

Table 1
Typical material properties for high modulus carbon fiber materials

Material property	Fiber	Laminate
Ultimate strain	0.004	0.0033
Tensile modulus of elasticity (GPa)	630	450
Ultimate strength (MPa)	2620	1540
Fiber volume fraction (%)	N/A	71

HM CFRP strips are typically bonded to the tension flange of steel–concrete composite beams using a structural epoxy adhesive. Six different adhesives were evaluated for use in bonding the HM strips to steel using scaled steel flexural specimens [6]. Of the adhesives studied, SP Systems Spabond 345 epoxy adhesive required the shortest development length to develop the full capacity of the HM CFRP strips. This adhesive was subsequently used for a series of scaled steel–concrete composite beam tests at NC State University.

3. Installation guidelines

Proper installation of the HM CFRP materials is critical to ensure proper performance of the strengthening system. Installation of externally bonded HM CFRP strips by adhesive bonding requires a multi-step approach. This includes preparation of the HM CFRP strips, preparation of the steel surface, application of the adhesive and installation of the strips. The different steps of the installation process are summarized in the following sections.

3.1. Preparation of the CFRP strips

Before commencing the surface preparation, the HM CFRP strips should be cut to length and have their ends detailed in accordance with the design of the adhesive joint. The design of the adhesive joint is governed by stresses that are critical near the ends of the HM CFRP strip. Several researchers have demonstrated that significant performance increases can be achieved by reverse tapering the thickness of the CFRP material at the ends as shown in Fig. 1(a). The previously reported research indicates that considerable performance enhancement can be achieved using this detail for members subjected to both static and fatigue loading conditions [9,10]. A reverse taper of 10–20° can be easily fabricated using a mechanical sander and sanding in the direction of the fiber, as shown in Fig. 1(b).

It is preferable that the HM CFRP strip be fabricated with a removable peel-ply and a pre-roughened surface on both sides of the strip to minimize the surface preparation of the HM CFRP strip. The peel-ply should be

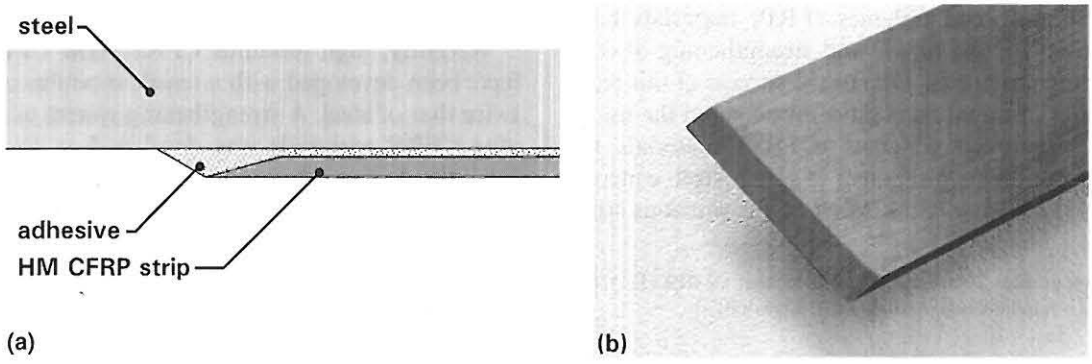

Fig. 1. Configuration of a 20° reverse tapered end.

removed immediately before bonding, to prevent possible contamination of the surface. If a peel-ply is not available for the HM CFRP strips, the strips should be lightly abraded with sandpaper on the side to be bonded and cleaned with a solvent, such as methanol [11].

3.2. Preparation of the steel surface

Surface preparation of the steel must be undertaken to ensure complete chemical bonds between the steel and the adhesive. This typically involves the removal of surface paint, mill scale, rust and surface cleaning [12]. The most effective way of achieving a chemically active surface is by grit blasting [13]. Grit blasting procedures use angular grit to remove the inactive oxide and hydroxide layers on the surface of the steel by cutting and deformation of the base material. In general, the grit should be angular, hard, properly graded, dry, and free of contaminants. Before grit blasting, the steel surface should be completely free from oils or other contaminants. Acetone, or a solvent suitable to remove the particular contaminant, should be used to remove these contaminants. Sanding or grinding the steel should be avoided since this process leaves the surface of the steel smooth and can redistribute contaminants into the surface.

Grit blasting should be completed until a "white metal" surface with a rough texture is achieved. Particular attention should be given to the steel near to where the ends of the strip will be bonded, since the stresses in the adhesive will be highest in this region. After grit blasting, any surface dust should be removed by brushing, vacuuming or blowing with a clean uncontaminated air supply. A final solvent cleaning after grit blasting may be completed; however, environmental constraints may limit the use of solvents. Application of the HM CFRP strips should take place as soon as possible after the surface preparation, preferably within 24 h, to minimize oxidation and recontamination of the surface.

3.3. Application of the adhesive and installation of the strips

The thickness of the adhesive bond line can affect the shear and peeling stresses that develop in the bond, particularly at the end of the adhesive joints. Thin bond lines result in higher stresses in the adhesive at the ends of the strip. In general, metal and FRP joints should have a target thickness of 0.5–2.0 mm [14]. For the specific case of steel–concrete composite beams strengthened with HM CFRP strips, adhesive thicknesses ranging between 0.1 and 1.0 mm have been successfully used for beams that were tested under static and fatigue loading conditions [7]. The appropriate adhesive thickness can be achieved using specially shaped trowels to spread the adhesive onto the surfaces. Additionally, non-metallic bond line spacer beads can be mixed with the adhesive to achieve the desired bond line thickness. The final thickness of the adhesive layer should be within the guidelines established by the designer since this thickness will greatly affect the bond stresses. The strip, with adhesive on one side, should be firmly pressed onto the steel surface and clamped in place within the pot-life of the adhesive to ensure adequate spreading of the adhesive.

4. Proposed design guidelines

There are several potential failure modes for a steel beam strengthened with FRP materials, such as failure by rupture of the FRP material, debonding of the FRP material, buckling of the compression flange and shear failure of the web [15]. For steel–concrete composite beams, crushing of the concrete in compression must also be considered. Of particular interest in this paper, are the failure modes by FRP rupture and FRP debonding. The remaining failure modes are failure modes for unstrengthened steel–concrete composite beams, and can be addressed using current design practices, after considering the effect of the increased load acting on the member due to the presence of the FRP material.

4.1. Design for flexure

Installation of HM CFRP materials can increase the elastic stiffness of a steel beam therefore reducing the elastic strain in the tension flange of the beam as compared to an unstrengthened beam at the same load level. Due to these two effects, the live load capacity of a steel beam can be increased using externally bonded CFRP materials. The following sections present a proposed design philosophy and design procedure that can be used to design the HM CFRP strengthening for steel–concrete composite flexural members to achieve a desired increase of the live load level of the member.

4.1.1. Design philosophy

The allowable increase of live load for a steel–concrete composite beam strengthened with HM CFRP materials should be selected to satisfy three conditions. These three conditions are shown in Fig. 2 with respect to the typical load–deflection behavior of a strengthened beam. Due to the presence of the additional HM CFRP material, the flexural yield load of the strengthened beam, $P_{Y,S}$, is greater than the flexural yield load of the unstrengthened beam, $P_{Y,US}$. The yield load of the strengthened and unstrengthened beams is defined as the load corresponding to yielding of the extreme fiber of the tension flange of the steel beam in both cases. To ensure that the strengthened member remains elastic under the effect of the increased live load, the total service load level of the strengthened beam, including the dead load, P_D, and the increased live load, P_L, should not exceed 60% of the calculated increased yield capacity of the strengthened beam. It should be noted that the increase of the yield load of the beam due to the presence of the HM CFRP materials is highly dependent on the level of the dead load acting on the unstrengthened mem-

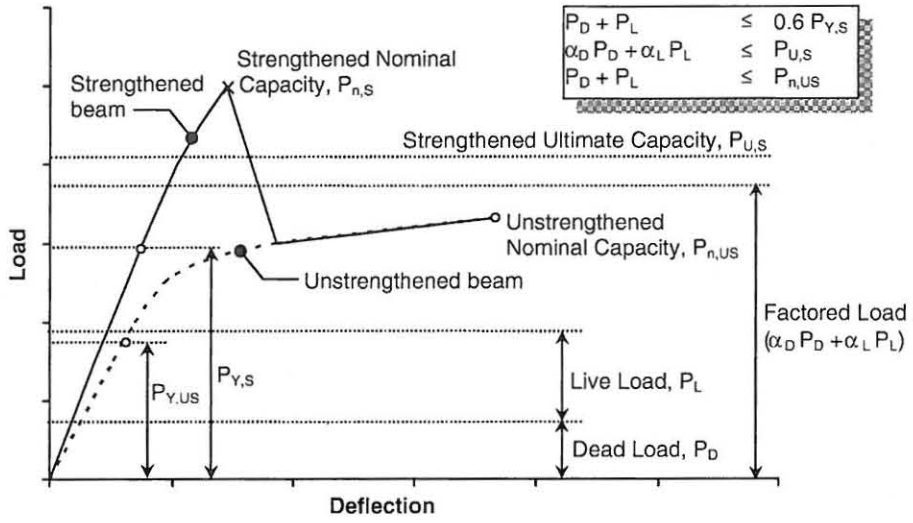

Fig. 2. Conditions for calculation of the allowable live load for a steel–concrete composite beam strengthened with HM CFRP materials.

ber prior to installation of the strengthening system. To satisfy the ultimate strength requirements, the total factored load based on the appropriate dead load and live load factors, α_D and α_L, respectively, should not exceed the ultimate capacity of the strengthened beam, $P_{U,S}$ after applying an appropriate strength reduction factor. Also, to ensure that the structure remains safe in case of possible loss of the strengthening system, the total load, including the dead load and the increased live load should not exceed the residual capacity of the unstrengthened beam, $P_{n,US}$. The fatigue life of the strengthened member under the effect of the increased live load level should be checked according to the fatigue design provisions of the applicable design codes. Based on a limited fatigue study, it was shown that the HM CFRP strengthening system can sustain an increase of the live load level corresponding to a stress range at the tension flange of the steel beam of 30% of the yield strength of the steel ($0.3f_y$) [7]. At this stress range, the fatigue durability of the strengthening system was comparable to that of an unstrengthened beam that was tested using the same stress range.

4.1.2. Design procedure

The design of the HM CFRP strengthening for a steel–concrete composite beam is conducted using a moment–curvature analysis. This analysis is based on the cross-sectional geometry as well as the stress–strain behavior of the constituent materials using the principal of strain compatibility. Thus, the moment curvature analysis should be conducted using a non-linear constitutive model for the concrete. A detailed description of the procedure is available in other sources [6,7].

The moment–curvature behavior of a given cross-section is determined based on the strain at the top level of the compression flange, ε_c, as shown in Fig. 3 together with an assumed neutral axis depth, c. The cross-section is divided into levels corresponding to the concrete deck, the longitudinal steel reinforcement of the concrete deck, the flanges and web of the steel beam, and the HM CFRP strips. For each level the strain can be determined based on compatibility of strains and horizontal force equilibrium. The effect of pre-applied dead loads, which act on the structure prior to installation of the HM CFRP strips, can be accounted for using the principle of superposition. Similarly, the effect of any prestress applied to the strips prior to installation can be accounted for in a similar manner.

From the strain profile and the constitutive relationships of the materials, the stress profile for the beam can be established as shown in Fig. 3. Integration of the stress profile provides the resultant forces of the different compo-

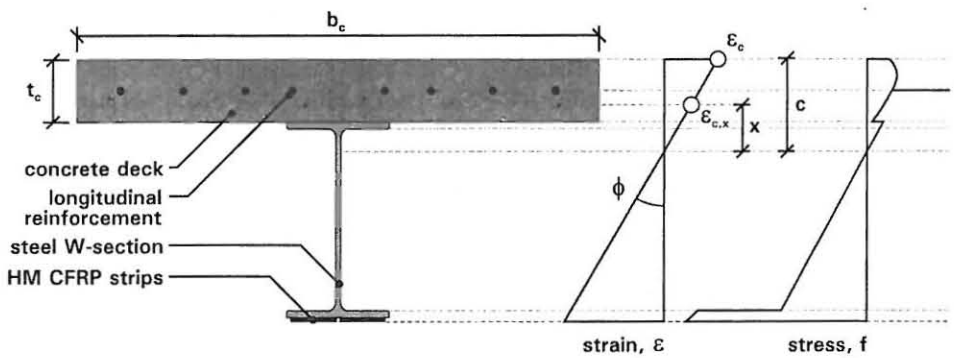

Fig. 3. Strain and stress profile for steel–concrete composite section strengthened with HM CFRP strips.

nents of the cross-section. For example, for the concrete deck, the strain, stress and force can be determined as:

$$\varepsilon_{c,x} = \phi x \tag{1}$$

$$f_c = \frac{f'_c n(\varepsilon_{c,x}/\varepsilon'_c)}{n - 1 + (\varepsilon_{c,x}/\varepsilon'_c)^{nk}} \tag{2}$$

$$F_c = b_c \int_{c-t_c}^{c} f_c(x)\,dx \tag{3}$$

where: $\varepsilon_{c,x}$ is the strain in the concrete deck at a distance x from the neutral axis; ϕ is the curvature of the section; f_c is the stress in the concrete deck at a distance x from the neutral axis; f'_c is the peak concrete stress measured from cylinder tests; ε'_c is the concrete strain at peak stress; n is the curve fitting factor; k is the post-peak decay factor; F_c is the resultant force in the concrete deck; b_c is the width of the concrete deck; c is the neutral axis depth; and t_c is the thickness of the concrete deck.

If the complete concrete stress distribution is measured for a representative concrete cylinder, the stress distribution defined by Eq. (2) can be established using a best-fit curve to the measured data. Alternatively, if only the concrete cylinder compressive strength, f'_c, is known, the remaining coefficients can be calculated using the equations provided by Collins and Mitchell [16]. The strain, stress and force resultants for the various other components can be calculated similarly using the appropriate constitutive models for the materials.

Horizontal force equilibrium can be achieved by several iterations of the neutral axis location. Once horizontal force equilibrium is satisfied, the nominal moment and corresponding curvature of the section can be calculated. The top surface strain can then be increased to determine the next increment of curvature and the procedure repeated. Using this technique, the full moment–curvature diagram can be obtained. The ultimate capacity of the section will be governed by rupture of the HM CFRP strips when the strain at the level of the CFRP reaches its limiting value.

To account for the statistical variability of the material properties of the composite system, ACI 440.2R-02 recommends that the mean strength of the FRP materials, $\bar{f}_{FRP,u}$, be reduced by three times the standard deviation, σ, for design purposes [17]. ACI 440.2R-02 further recommends that the strength of the FRP system be reduced by an environmental reduction factor, C_E (equal to 0.85 for CFRP materials), to account for possible degradation of the composite materials. Thus, the design ultimate strength of the CFRP materials, $f_{FRP,u}$, can be given by:

$$f_{FRP,u} = 0.85(\bar{f}_{FRP,u} - 3\sigma) \tag{4}$$

The design ultimate strain can be calculated by dividing the design ultimate strength by the modulus of elasticity of the HM CFRP material.

The load–deflection behavior for a given beam and loading configuration can be determined by integration of the curvature profile, $\phi(x)$, using any commonly accepted technique as shown schematically in Fig. 4 for a simply supported beam loaded by two symmetric concentrated loads. Once the nominal capacity of the strengthened member, is established, the design ultimate capacity can be determined by applying an appropriate reduction factor, ϕ. To account for the brittle nature of failure associated with rupture of the CFRP materials, a reduction factor, ϕ, of 0.75 is proposed which is consistent with the reduction factor used by the American Institute of Steel Construction (AISC) for rupture type limit states [18].

4.2. Design for bond

The preceding analysis was based on the cross-section of the member alone, and assumed that a perfect bond exists between the steel and the HM CFRP strips. While this assumption is sufficient to predict the flexural behavior of the strengthened member up to the ultimate tensile strength of the HM CFRP material, a premature debonding failure will limit the capacity of the section. Furthermore, debonding failures occur suddenly and without warning and consequently considerable care must be taken to avoid this type of failure.

An analytical procedure was developed for determining bond stresses for a beam strengthened with externally

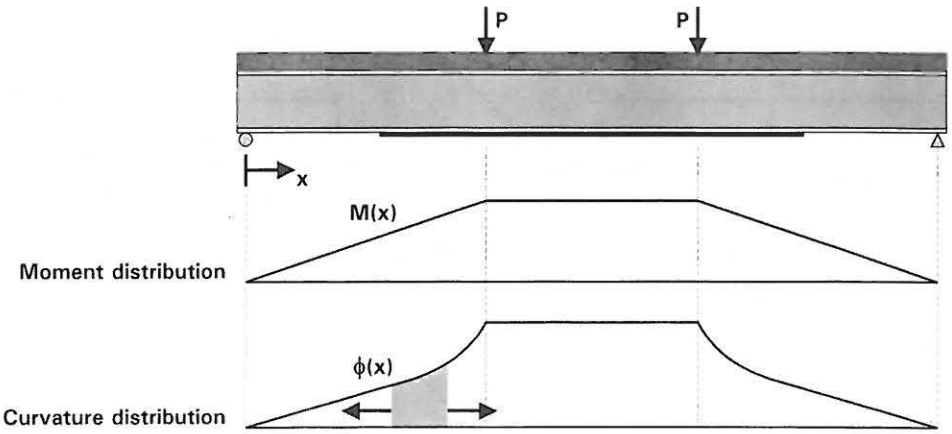

Fig. 4. Calculation of deflection by integration of the curvature profile.

bonded CFRP materials [6]. The analysis includes the effect of the applied loading, the thermal effects resulting from differing coefficients of thermal expansion, as well as any prestressing applied to the CFRP strip before bonding. The following sections describe the design philosophy and the procedure to determine the bond stresses in an adhesive joint.

4.2.1. Design philosophy

Bond stresses in the adhesive joint arise from both shear stresses and peeling stresses which result from the transfer of stresses between the steel beam and the bonded FRP material. Due to the complexity of the stress distribution, it is insufficient merely to consider the average shear stress in the joint when analyzing the adequacy of an adhesive system. To properly design the adhesive joint, the maximum shear and peeling stresses, which occur at the end of the strips, should be considered. Based on these stresses, the maximum principle stress in the joint can be determined and compared to the characteristic strength of the adhesive system.

4.2.2. Design procedure

The strength of an adhesive system must be determined empirically since this strength depends not only upon the properties of the substrates and adhesives, but also upon the degree of surface preparation that is expected. The characteristic strength of an adhesive system can be determined from lap-shear tests [13]. The same materials and bonding techniques should be used in the preparation of the lap-specimens as those used in the actual strengthening operation. This will help to ensure that the results of the lap tests are representative of the actual behavior of the system. The appropriate lap-splice theory can be employed to calculate the maximum shear and peeling stresses at the end of the bonded region at the time of failure. The characteristic strength, σ_c, of the adhesive system can be calculated as,

$$\sigma_c = \frac{\sigma}{2} + \sqrt{\left(\frac{\sigma}{2}\right)^2 + \tau^2} \tag{5}$$

where σ is the maximum peeling stress in the lap-splice and τ is the corresponding maximum shear stress. The calculated characteristic strength represents the strength that should be used for design of the actual beam including any safety factors. Safety factors have been proposed for the joining of FRP materials that take into account the uncertainties in preparing an adhesive joint as well as the changes in material properties over time [14].

If the same system is to be used for strengthening of an actual member, the characteristic strength can be compared to the bond stresses determined for the strengthened beam. The first step is to determine the distribution of shear stress and peeling stress along the length of the CFRP strip. For a steel–concrete composite beam strengthened with a CFRP strip or any other FRP material with untapered ends and loaded in four-point bending as shown in Fig. 5, the shear stress distribution is given by,

$$\tau(x) = \begin{cases} B_1 \cosh(\lambda x) + B_2 \sinh(\lambda x) + m_1 P & 0 \leqslant x \leqslant (b-a) \\ B_3 \cosh(\lambda x) + B_4 \sinh(\lambda x) & (b-a) \leqslant x \leqslant L_{frp}/2 \end{cases} \tag{6}$$

where

$$\lambda^2 = \frac{G_a b_{frp}}{t_a}\left[\frac{(y_s + y_{frp})(y_s + y_{frp} + t_a)}{E_s I_s + E_{frp} I_{frp}} + \frac{1}{E_s A_s} + \frac{1}{E_{frp} A_{frp}}\right]$$

$$m_1 = \frac{G_a}{t_a \lambda^2}\left(\frac{y_s + y_{frp}}{E_s I_s + E_{frp} I_{frp}}\right)$$

$$B_1 = \frac{-G_a}{t_a \lambda}\left[(\alpha_{frp} - \alpha_s)\Delta T - \frac{y_s}{E_s I_s} Pa\right] - m_1 P e^{-k}$$

$$B_2 = \frac{G_a}{t_a \lambda}\left[(\alpha_{frp} - \alpha_s)\Delta T - \frac{y_s}{E_s I_s} Pa\right]$$

$$B_3 = \frac{-G_a}{t_a \lambda}\left[(\alpha_{frp} - \alpha_s)\Delta T - \frac{y_s}{E_s I_s} Pa\right] + m_1 P \sinh(k)$$

$$B_4 = \frac{G_a}{t_a \lambda}\left[(\alpha_{frp} - \alpha_s)\Delta T - \frac{y_s}{E_s I_s} Pa\right] - m_1 P \sinh(k)$$

$$k = \lambda(b - a)$$

$A_{s,FRP}$ is the cross-sectional area; $E_{s,FRP}$ is the tensile modulus of elasticity; $I_{s,FRP}$ is the moment of inertia; $y_{s,FRP}$ is the distance to the centroid from the bottom of the steel

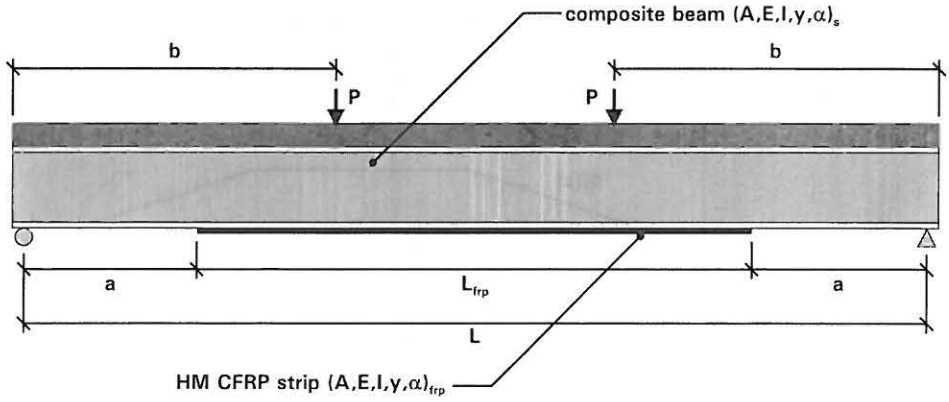

Fig. 5. Beam configuration for bond stress equations.

section; $\alpha_{s,FRP}$ is the coefficient of thermal expansion; b_{FRP} is the width of the FRP strip; G_a is the shear modulus of the adhesive; t_a is the adhesive thickness; ΔT is the temperature change; x is the distance from the end of the FRP strip to the location at which the stresses are being calculated; a, b, L, L_{FRP} and P are as defined in Fig. 5. The subscripts 's' and 'FRP' refer to the transformed properties of the steel–concrete composite beam and the FRP strip, respectively.

A detailed derivation of the expressions in Eq. (6) is provided by Schnerch [6]. The distribution of the peeling stresses along the length of the CFRP strip can be calculated using the equations presented by Smith and Teng [19]. While the equations are complex, they are of a closed form and can be easily solved using available computer software.

Once the shear and peel stress distributions are known, the maximum principle stress, which will typically occur near the end of the joint, can be calculated using Eq. (5). To ensure that the capacity of the bonded joint is adequate, the maximum principle stress in the joint should not exceed the characteristic strength of the bonding system including the appropriate safety factors.

5. Worked example

To demonstrate the application of the design principles described in this paper, the analysis of a typical strengthened steel–concrete composite beam was considered. The details of the example beam, including the geometric and material properties, are given in Fig. 6. The complete stress–strain relationship of the concrete in the compression zone of the beam is defined in terms of the measured cylinder compressive strength using Eq. (2) [16]. The constants presented in Fig. 6 were determined to provide a best fit of the measured stress–strain curve for a series of representative concrete cylinders. An elastic–perfectly plastic material model was used to represent the structural steel W-section and the longitudinal reinforcement as shown in Fig. 6. The linear-elastic material model used for the HM CFRP material is also shown in Fig. 6.

This beam was also tested to failure at NC State University to examine the reliability of the proposed design guidelines. Details of the example beam test can be found in Schnerch [6]. The moment–curvature relationship of the strengthened beam was calculated at the service load level and at the ultimate level based on the proposed design procedure. The moment–curvature relationship was extended to predict the load–deflection behavior of the example beam.

5.1. Moment–curvature relationship

Under service loading conditions the total effect of the dead load and the increased live load should not exceed 60% of the increased yield strength of the strengthened beam. This corresponds to a maximum strain in the tension flange of the strengthened beam of 0.00105. Since the section remains elastic under service loading conditions, the neutral axis depth coincides with the centroid of the transformed section. The curvature of the section under service loading conditions is 4.1×10^{-6} rad/mm. From the known curvature and the strain at the bottom of the steel section and using the appropriate material models, given in Fig. 6, the resultant forces for the concrete deck, the longitudinal reinforcing steel, the steel section and the HM CFRP strips were calculated and horizontal force equilibrium was verified. The calculated nominal moment of the section at the service load level is 286 kN m.

The moment–curvature analysis was also conducted to predict the nominal capacity of the example beam. The experimental results of the beam test indicate that failure of the beam occurred due to rupture of the HM CFRP strips when the strain at the level of the HM CFRP reached the mean rupture strain reported by the manufacturer of 0.0033 [6]. The corresponding applied moment immediately prior to failure was 663 kN m. Based on the proposed moment–curvature analysis, the moment capacity of the section corresponding to a strain of 0.0033 at the level of the CFRP strips was calculated as 674 kN m, which correlates well with the measured experimental results. However, based on the provisions in the proposed guidelines, the nominal capacity of the section is calculated when the strain at the level of the FRP reaches the design ultimate strain, $\varepsilon_{FRP,u}$. Based on Eq. (4) and the average modulus of elasticity of the CFRP $\varepsilon_{FRP,u}$ was calculated as 0.0027. By iteration of the neutral axis depth until force equilibrium is satisfied, the neutral axis is found to be 149 mm below the top surface of the concrete deck. The corresponding curvature of the section is 10.1×10^{-6} rad/mm. The calculated nominal moment capacity of the section is 606 kN m. Therefore, the ultimate moment capacity of the section based on a strength reduction factor, ϕ, of 0.75 is calculated as 455 kN m.

The moment and curvature of the section were calculated for several points prior to rupture of the CFRP. The predicted and measured moment–curvature relationships are compared in Fig. 7. Inspection of the figure demonstrates that the calculated moment and curvature of the section accurately predict the measured values. The slight deviation after yielding, which can be seen in the figure, reflects the effect of the residual stresses that form in the steel section during the manufacturing process [7]. It should be noted that the calculated nominal capacity of the strengthened section, $M_{n,S}$, which is used for design purposes is lower than the measured capacity determined experimentally which demonstrates that the proposed design method is conservative. The ultimate capacity of the section and the service moment calculated according to the proposed design guidelines are also shown in the figure for reference purposes.

5.2. Load–deflection relationship

The load–deflection response of the example beam was established by numerical integration of the curvature of

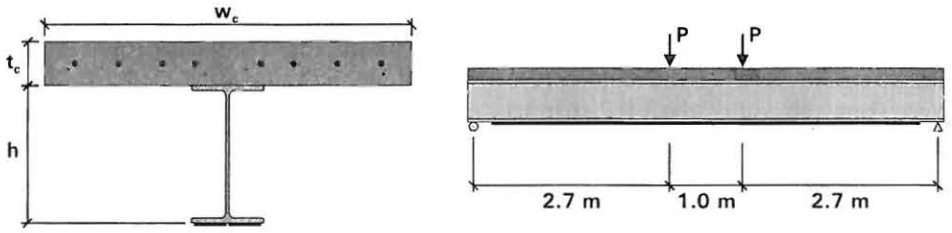

Geometric Properties

Concrete Deck		***FRP Strip***	
Width, w_c	= 840 mm	Width, w_{FRP}	= 150 mm
Thickness, t_c	= 100 mm	Thickness, t_{FRP}	= 4 mm
Longitudinal Reinf.		***Steel W-Section (W310 x 45)***	
Area, A_s	= 1000 mm^2	Width, w	= 165 mm
Distance from top, d_s	= 50 mm	Height, h	= 315 mm
		Flange Thickness, t_f	= 10 mm
		Web thickness, t_w	= 7.0 mm

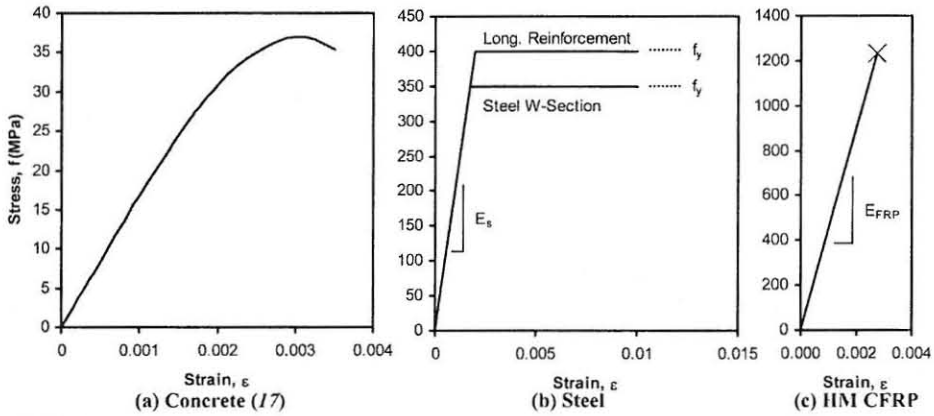

Material Properties

Concrete		***Steel W-Section***	
Cylinder strength, f_c'	= 37.0 MPa	Modulus of Elasticity, E_s	= 200 GPa
Strain at peak stress, ε_c'	= 0.0031	Yield strength, f_y	= 360 MPa
Failure strain, ε_{cu}	= 0.0035	***Longitudinal Reinf.***	
Curve fitting factor, n	= 3.27	Modulus of Elasticity, E_s	= 200 GPa
Post peak factor, k	= 1.00 $\varepsilon_c < \varepsilon_c'$	Yield strength, f_y	= 400 MPa
	= 1.23 $\varepsilon_c > \varepsilon_c'$	***FRP Strip***	
		Modulus of Elasticity, E_{FRP}	= 450 GPa
		Average strength, $\overline{f}_{FRP,u}$	= 1543 MPa
		Standard deviation, σ	= 30 MPa

Fig. 6. Details of the example beam.

the section up to the calculated nominal capacity of the strengthened beam which corresponds to, $P_{n,S}$, of 449 kN. The load–deflection behavior of the unstrengthened beam up to crushing of the concrete, which corresponds to $P_{n,US}$ of 332 kN, was also calculated using a similar procedure. The predicted load and deflection of the strengthened and unstrengthened beams are presented in Fig. 8. The service load level, $P_D + P_L$, the factored load including the increased live load, $\alpha_D P_D + \alpha_L P_L$ and the ultimate capacity of the strengthened beam, $P_{U,S}$, are also shown in Fig. 8. The factored load was calculated based on the AASHTO Strength I limit state with live load and dead load factors of 1.75 and 1.25, respectively [20]. The self-weight of the structure was assumed to be 30% of the calculated yield load of the unstrengthened beam, $P_{Y,US}$. As seen in Fig. 8, the increased live load level for the strengthened beam, calculated using the proposed procedure, satisfies the three conditions discussed previously. Particularly,

$$P_D + P_L = 212\ \text{kN} = 0.6P_{Y,S}$$

$$\alpha_D P_D + \alpha_L P_L = 335\ \text{kN} < P_{U,S} = 337\ \text{kN}$$

$$P_D + P_L = 212\ \text{kN} < P_{n,US} = 332\ \text{kN}$$

The service load level for the unstrengthened beam was calculated to be 143 kN. Therefore, using the HM CFRP strengthening system resulted in a 50% increase of the service load level of the beam.

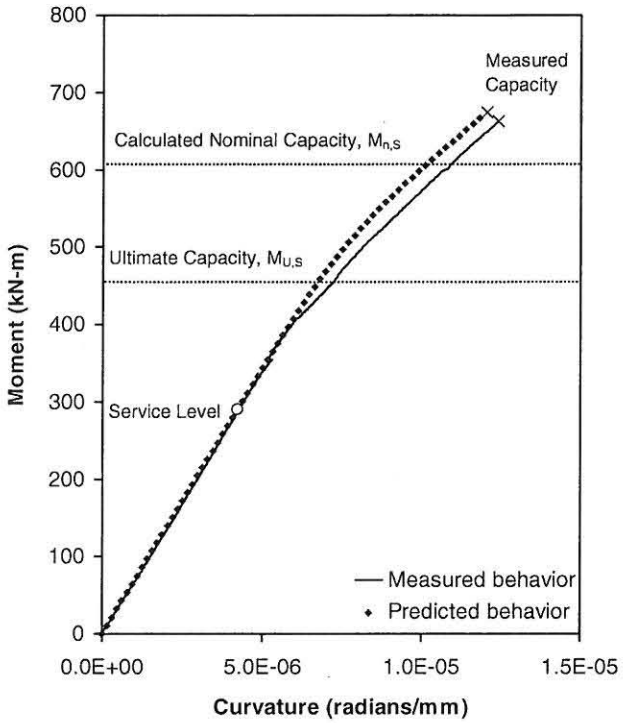

Fig. 7. Comparison of the predicted and measured moment–curvature behavior.

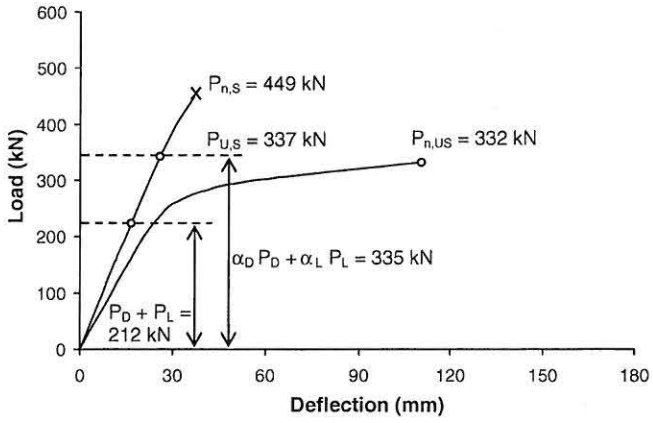

Fig. 8. Load–deflection behavior of the example beam.

6. Conclusions

This paper presented installation and structural design guidelines that can be used by practitioners for the proper installation, analysis and design of HM CFRP materials to strengthen and repair steel–concrete composite bridge girders. Proper installation is critical to ensure that the strengthened member behaves as intended by the designer. Simplified analytical tools can be used to determine the flexural behavior of the strengthened beam and to design the geometric configuration and required material properties of the HM CFRP materials. The design should be based on an allowable increase of the live load level. The increased live load level for the strengthened beam should satisfy three conditions. The combined effect of the dead load and the increased live load should not exceed 60% of the increased yield strength of the strengthened beam. Also, the factored load acting on the girder should not exceed the ultimate capacity of the strengthened member. Finally, the total increased service load acting on the structure should not exceed the ultimate capacity of the unstrengthened beam. The proposed design procedures accurately predicted the behavior of a steel–concrete composite beam strengthened with HM CFRP materials. To prevent debonding of the HM CFRP strips, it is important to consider the actual state of stress near the end of the strip including shear and peeling stress components. High modulus CFRP materials are an effective alternative to conventional strengthening techniques, including bolting and welding of steel plates, for steel–concrete composite bridge girders.

Acknowledgements

The authors acknowledge the National Science Foundation (NSF) Grant EEC-0225055, the NSF Industry/University Cooperative Research Center (I/UCRC) for the Repair of Buildings and Bridges with Composites (RB^2C) and Mitsubishi Chemical FP America.

References

[1] Mertz DR, Gillespie Jr. JW, Rehabilitation of steel bridge girders through the application of advanced composite materials. Contract NCHRP-93-ID011, Transportation Research Board; 1996.
[2] Sen R, Libby L, Mullins G. Strengthening steel bridge sections using CFRP laminates. Compos Part B: Eng 2001;39:309–22.
[3] Tavakkolizadeh M, Saadatmanesh H. Repair of damaged steel–concrete composite girders using carbon fiber-reinforced polymer sheets. J Compos Construct 2003;7(4):311–22.
[4] Tavakkolizadeh M, Saadatmanesh H. Strengthening of steel–concrete composite girders using carbon fiber reinforced polymer sheets. J Struct Eng 2003;129(1):30–40.
[5] Al-Saidy AH, Klaiber FW, Wipf TJ. Repair of steel composite beams with carbon fiber-reinforced polymer plates. J Compos Construct 2004;8(2):163–72.
[6] Schnerch D. Strengthening of steel structures with high modulus carbon fiber reinforced polymer (CFRP) materials. PhD dissertation, North Carolina State University, Raleigh (NC); 2005.
[7] Dawood M. Fundamental behavior of steel–concrete composite beams strengthened with high modulus carbon fiber reinforced polymer (CFRP) materials. Master's thesis, North Carolina State University, Raleigh (NC); 2005.
[8] Schnerch, D., Dawood, M., Rizkalla, S., 2005. Design Guidelines for the Use of HM Strips: Strengthening of Steel-Concrete Composite Bridges with High Modulus Carbon Fiber Reinforced Polymer (CFRP) Strips. Technical Report No. IS-06-02. North Carolina State University.
[9] Hildebrand M. Non-linear analysis and optimization of adhesively bonded single lap joints between fibre-reinforced plastics and metals. Int J Adhes 1994;14(4):261–7.
[10] Allan RC, Bird J, Clarke JD. Use of adhesives in repair of cracks in ship structures. Mater Sci Technol 1998;4:853–9.
[11] Hollaway LC, Cadei J. Progress in the technique of upgrading metallic structures with advanced polymer composites. Prog Struct Eng Mater 2002;4(2):131–48.

[12] Mays GC, Hutchinson AR. Adhesives in civil engineering. New York: Cambridge University Press; 1992.
[13] Cadei JMC, Stratford TJ, Hollaway LC, Duckett WG. Strengthening metallic structures using externally bonded fibre-reinforced polymers. Publication C595, Construction Industry Research and Information Association (CIRIA), London, UK; 2004.
[14] Institution of Structural Engineers. A guide to the structural use of adhesives, The Institution of Structural Engineers, London, UK; 1999.
[15] Buyukozturk O, Gunes O, Karaca E. Progress on understanding debonding problems in reinforced concrete and steel members strengthened using FRP composites. Construct Build Mater 2004;18(1):9–19.
[16] Collins MP, Mitchell D. Prestressed concrete structures. Canada: Response Publications; 1997.
[17] American Concrete Institute. ACI 440.2R-02 guide for the design and construction of externally bonded FRP systems for strengthening concrete structures; 2002.
[18] American Institute of Steel Construction. Manual of steel construction: load and resistance factor design, 3rd ed.; 2001.
[19] Smith ST, Teng JG. Interfacial stresses in plated beams. Eng Struct 2001;23:857–71.
[20] AASHTO LRFD Bridge Design Specifications. American Association of State Highway and Transportation Officials, Washington (DC); 2002.